

RESEARCH PAPER



# TRIM13 inhibits cell proliferation and induces autophagy in lung adenocarcinoma by regulating KEAP1/NRF2 pathway

Bo Yu<sup>a</sup>, Yu Zhou<sup>b</sup>, and Jinxi He<sup>a</sup>

<sup>a</sup>Department of thoracic surgery, The General Hospital of Ningxia Medical University, Yinchuan, Ningxia, China; <sup>b</sup>Department of Scientific Research, The General Hospital of Ningxia Medical University, Yinchuan, Ningxia, China

## ABSTRACT

Lung adenocarcinoma (LUAD) is the most common type of lung cancer. Tripartite motif 13 (TRIM13) is a member of TRIM protein family and is downregulated in multiple cancers, especially non-small cell lung cancers (NSCLC). In this study, we investigated anti-tumor mechanism of TRIM13 in non-small cell lung cancer tissues and cell lines. First, the mRNA and protein levels of TRIM13 in LUAD tissue and cells were measured. TRIM13 was overexpressed on LUAD cells to investigate the effects on cell proliferation, apoptosis, oxidative stress, p62 ubiquitination, and autophagy activation. Finally, mechanistic role of TRIM13 in regulating the Keap1/Nrf2 pathway was investigated. Results indicated that low level of TRIM13 mRNA and protein expression was found in LUAD tissue and cells. Overexpression of TRIM13 in LUAD cancer cells suppressed their proliferation, increased apoptosis, and oxidative stress, ubiquitinated p62, and activated autophagy via the RING finger domain of TRIM13. Furthermore, TRIM13 showed interaction with p62 and mediated its ubiquitination and degradation in LUAD cells. Mechanistically, TRIM13 exerted the tumor suppressor functions in LUAD cells by negatively regulating Nrf2 signaling and downstream antioxidants, which was further confirmed by *in vivo* data from xenografts. In conclusion, TRIM13 behaves like a tumor suppressor and triggers autophagy in LUAD cells by mediating p62 ubiquitination via KEAP1/Nrf2 pathway. Our findings provide a novel insight into targeted therapy plans for LUAD.

## ARTICLE HISTORY

Received 15 January 2023  
Revised 21 March 2023  
Accepted 22 March 2023



## KEYWORDS


Lung adenocarcinoma;  
TRIM13; autophagy;  
ubiquitination; oxidative  
stress

## 1. Introduction

Lung cancer (LC) is ranked as one of the leading causes of death worldwide and causes almost one-quarter of all deaths in both sexes [1]. Histologically, LC can be divided into two main types with different treatment strategies, small-cell lung cancer (SCLC) and non-small cell lung cancer (NSCLC). The most common histological subtype of NSCLC is lung adenocarcinoma (LUAD). Although significant advances have been made to treat LUAD such as surgery, radiotherapy, chemotherapy, targeted therapy, and immunotherapy, yet survival rate of these patients remains low [2]. Currently, imaging examination is effective in screening patients, but it is ineffective for early-stage detection of adenocarcinoma [3,4]. Furthermore, the prognosis remains poor in the advanced stage of NSCLC in patients treated with standard chemotherapy [5]. Hence, understanding disease mechanisms and the development of new therapeutic targets is urgently warranted.

Autophagy is a conserved physiological process that is activated under cellular stress or nutrient depletion condition [6,7]. It is a double-edged sword with both tumor suppressor and tumor promoter activities. Autophagy mediates tumor suppression via many protective mechanisms such as inhibiting ROS accumulation and DNA damage, preventing genomic instability, and clearing oncogenic proteins [8] that increase cell survival and its prolonged activation results in autophagy-mediated cell death [9]. Notably, abnormalities in autophagy have been associated with an enhanced risk of malignancy. Tumor suppressor proteins such as PTEN and Liver kinase B1 are activators of autophagy [10], conversely, oncoproteins such as PI3K and Akt1 are potential inhibitors of this pathway [11]. Additionally, controlled activation of autophagy inhibits cell proliferation and stimulates cell death in Huh7 HCC cells [12]. Atg4C is a protease that senses ROS level in autophagic machinery and

**CONTACT** Jinxi He  [nypxwk@163.com](mailto:nypxwk@163.com)  Department of thoracic surgery, The General Hospital of Ningxia Medical University, No. 804 South Victory Street, Yinchuan, Ningxia 750004, China

 Supplemental data for this article can be accessed online at <https://doi.org/10.1080/15384101.2023.2216504>

enables the formation of autophagosome via LC3/Atg8 [13]. Defects in autophagy have been reported to be associated with the development of neurodegenerative diseases of nervous system [14,15] and cancers [16–18]. Thus, autophagy acts as a tumor suppression mechanism and limits cell growth and genomic instability [19]. However, some findings indicate that autophagy also promotes oncogenesis. For instance, increased autophagy level is observed in tumor cells with activated Ras oncogene [20]. Moreover, autophagy breakdowns cytoplasm and provides nutrients to cancer cells. It also promotes the survival of metastatic cells during detachment [21]. Multiple other studies indicate autophagy as a mechanism to facilitate tumors [17,22]. Taken together, the role of autophagy in cancer is context-dependent and may act as a tumor suppressor or tumor promoter.

*TRIM13* is a member of the tripartite motif (TRIM) family, and its gene is located on the 13q14 chromosome. Members of the TRIM family have been reported to regulate multiple processes such as cell proliferation [23,24], cell metabolism [25], autophagy [26] and regulate gene expression [27,28]. Importantly, most of the members of this family are E3 ubiquitin ligase. Several target oncogenic proteins have been identified for ubiquitination by TRIM13 such as TARF6 (Tumor Necrosis Factor Receptor-Associated Factor 6), Akt, and MDM2 [26,29]. When TRIM13 is overexpressed, it leads to the ubiquitination and proteasomal degradation of MDM2 and AKT, resulting in increased p53 stability and decreased AKT kinase activity. Ultimately, this enhances the level of apoptosis induced by irradiation [29]. TRIM13 also downregulates NF- $\kappa$ B, which is essential for negative regulation of clonogenic ability of the cells [30]. It also plays a crucial role in protein degradation (ERAD) during ER stress via the ubiquitin-proteasome system [31]. Autophagy is a well-known mitigator of ER stress and facilitates the degradation of proteins, and even cell death during persistent ER stress [32]. TRIM13 cooperates with p62, a ubiquitin-binding adaptor protein, to regulate the ubiquitination mechanism [26]. Ubiquitin-proteasome pathway (UPP) is a crucial path for protein degradation and its dysfunction results in the development of multiple malignancies. A recent study showed that

TRIM13 is downregulated in NSCLC and its overexpression was found to inhibit NF- $\kappa$ B [33]. Importantly, overexpression of TRIM13 in NSCLC cell lines induced apoptosis and hampered tumor growth in the xenograft model suggesting its tumor-suppressive role [33]. Here, we demonstrate that TRIM13 is a tumor suppressor that induces autophagy in lung adenocarcinoma by regulating the Nrf2 pathway and mediating SQSTM1 (p62) ubiquitination. These new findings may open novel avenues for targeted therapy of LAUD.

## 2. Materials and methods

### 2.1. Patient specimens

A total of 20 fresh LUAD tissues and 20 matched normal lung samples were supplied from the Department of Thoracic Surgery, The General Hospital of Ningxia Medical University. The study was approved by research ethics Committee of the General Hospital of Ningxia Medical University and in accordance with the Basic & Clinical Pharmacology & Toxicology policy for experimental and clinical studies [34].

### 2.2. Cell lines and cell culture

Three LUAD cell lines (A549, NCI-H1650, and HCC827) and one normal human bronchial epithelial cell line (BEAS-2B) were purchased from ATCC (MD, USA). BEAS-2B cell line was cultured in BEGM growth medium, A549 cell line was grown in F-2K medium, while NCI-H1650 and HCC827 cell lines were supplemented with RPMI-1640 medium. All the cells were cultured with appropriate media and supplemented with 10% FBS, 100 U/ml penicillin, and 100  $\mu$ g/mL streptomycin. All cells were maintained in a humidified 5% CO<sub>2</sub> incubator at 37 degrees. A549 cells received treatment with or without 10 mM of MG132, a protein degradation inhibitor, for 6 h. These cells also received treatment with 50  $\mu$ g/mL cycloheximide (CHX), a protein synthesis inhibitor, at different time points.

### 2.3. RNA extraction and RT-qPCR

RNA from cells and tissues was extracted with GENEzol™ reagent (Geneaid) with the standard method. Briefly, samples were homogenized with GENEzol and separated using chloroform. Isopropanol was added to the separate aqueous phase, which is then centrifuged to obtain tight RNA pellets. These pellets were washed with 70% ethanol and finally resuspended in 50uL of RNase-free water. The RNA extracts were obtained with concentration greater than 500 ng per  $\mu\text{L}$  and RNA, 1.98  $A_{260}/A_{280}$  ratio. cDNA was prepared using reverse transcription kit (QuantiNova), and qPCR was performed on samples using Bio-Rad CFX96 machine according to the recommended protocol. The relative gene expression was analyzed by  $2^{-\Delta\Delta C_t}$  method that normalized to the internal control  $\beta$ -actin. The primers used to amplify TRIM13 were: Forward ATTGAAGATGCCTACGC TCG and Reverse: GTGAGTAACTGGAGGGC TTTC. P62 was: Forward GGTGAAGAACTGC TGTACAAAG and Reverse: CACACTTGGGCA CTGAGAG. NQO1 was: Forward: TGAAGAA GAGAGGATGGGAGG and Reverse: GATGACTC GGAAGGATACTGAAAG. For normalization, expression of  $\beta$ -actin was examined with the primer pair of forward: ACCTTCTACAATGAGCTGCG and Reverse: CTGGATGGCTACGTACATGG.

### 2.4. Immunohistochemistry (IHC)

Human LUAD tissue specimens ( $n = 3$ ), human normal lung tissue specimens ( $n = 3$ ), xenograft specimens from mice in the oe-NC, oe-TRIM13, and oe-TRIM13+oe-NRF2 groups ( $n = 5$  per group) were used in the IHC staining assay. For each specimen, at least three slices were used. PFA-fixed tissues were utilized to prepare paraffin-embedded blocks. A microtome machine was used to prepare 5um tissue sections on charged slides which were deparaffinized and rehydrated using xylene and alcohol. Tissue sections were boiled in the microwave at 95 degrees using 0.01 sodium citrate buffer (pH 6.5) to achieve antigen retrieval. Slides were stained using Novolink Polymer Detection System, which was then counterstained with hematoxylin, dehydrated, mounted, and finally covered with cover-slips. The primary antibodies included anti-TRIM13 (1:100, cat. no.

Ab234847; Abcam, Cambridge, MA, USA), anti-Ki67 (Novus, NB500–170), and anti-p62 (1:1000, cat. no. ab207305, Abcam). For each slide, at least five randomly selected fields were photographed under an OLYMPUS B $\times$ 51 microscope (Olympus, Tokyo, Japan). The staining results were analyzed by two independent pathologists using the ImageJ software to quantify the frequency of positive cells.

### 2.5. Western blot

Protein from cells and tissues was extracted using RIPA buffer containing protease and phosphatase inhibitors. Protein was then separated using SDS-PAGE and transferred to PVDF membranes. After blocking, membranes were incubated overnight in a cold chamber (4 degrees) with primary antibodies including anti-Bax (Abcam, 1/1000, ab32503), anti-Bcl-2 (Abcam, 1/1000, ab32124), anti-Cyclin A1 (Abcam, 1/1000, ab270940), anti-Cyclin D1 (Abcam, 1/100, ab16663), anti-HA (Abcam, ab9110), anti-Flag (Sigma-Aldrich, F1804), anti-Ub (Santa Cruz Biotechnology, sc8017), anti-TRIM13 (1:100, cat. no. Ab234847), anti-p62 (1:50, sc-48,402), anti- $\beta$ -actin (1:50 sc-47,778), anti-KEAP1 (Sigma, AV38981), anti-tubulin (Novus, NB100–690), and anti-H3 (Abcam, 1:1000, ab176842). The next day, membranes were washed with washing buffer and incubated with horseradish peroxidase (HRP)-conjugated secondary antibodies for 1 h at room temperature. Finally, bands were visualized and detected with an enhanced chemiluminescence kit (Abcam), and protein intensity was analyzed by the ImageJ software. Whole WB membranes have been provided in supplementary material, S1.

### 2.6. Cell transfection

The oe-TRIM13 and oe-TRIM13+oe-NRF2 lentiviral vectors and a non-targeting control vector oe-NC were provided by Hanbio Therapeutics (Shanghai, China). The oe-TRIM13-Flag, and oe-Nrf2 vectors were constructed using pcDNA3.1 following methodology of standard subcloning. TRIM13 mutant version with depletion of  $\Delta$ RING (TRIM13- $\Delta$ RING) was constructed using CRISPR/Cas9. The sgrNAs were designed by the CRISPR sgrNA design web tool, and the annealed

oligonucleotides were integrated into the pSpCas9n(BB)-2A-GFP vector (Addgene 48,140) [35]. The empty vector (oe-NC) was used as a negative control. Upon reaching 70% confluence A549 and HCC287 cells were transfected using Lipofectamine® 2000 at a final concentration of 20 nmol/l (Invitrogen Life Technologies, Carlsbad, CA, USA). Finally, cells were harvested after 48 hours.

## 2.7. Colony formation

A total of  $2 \times 10^3$  A549 and HCC287 cells were seeded into 6-well plates and culture for 2 wk. Colonies were fixed with 4% PFA and subsequently stained with 0.1% crystal violet for 15 min at room temperature. The colonies (>50 cells) were visualized using an OLYMPUS B×51 microscope and quantified with the ImageJ software.

## 2.8. Cell Counting Kit-8 (CCK-8)

Cell proliferation and viability were assessed by CCK-8 assay (Sigma: 96992) according to protocol. Briefly, A549 and HCC287 cells were plated in a 96-well tissue culture plate at a density of  $1 \times 10^4$  cells/well and maintained for 24 hours. Cell viability was evaluated by adding 100  $\mu$ L of CCK-8 solution (Dojindo, Japan) added to each well for 24 hours. The absorbance was measured at 450 nm using an ELISA microplate reader.

## 2.9. Apoptotic assay by flow cytometry

Apoptosis in cells was evaluated using an apoptosis staining kit (Beyotime, Shanghai, China) by flow cytometry (BD Biosciences, Franklin Lakes, NJ, USA). Briefly, A549 and HCC287 cells were seeded in 6-well culture plates at the density of  $2 \times 10^3$  cells/mL overnight. After digestion, cells were washed thrice with PBS and resuspended in a binding buffer. Cells were then incubated in darkness at room temperature in FITC-labeled Annexin V and PI for 15 min. The percentage of apoptotic cells was finally assessed by flow cytometry.

## 2.10. Transmission electron microscopy (TEM)

A549 cells were trypsinized, washed thrice with PBS, and fixed in 2.5% glutaraldehyde in 0.1 mol/L phosphate buffer (pH 7.2) overnight at 4°C. Cells were washed on the next day with 0.1 mol/L phosphate buffer and fixed in 1% aqueous osmium. After that, they were dehydrated with increasing concentrations of ethanol and finally embedded in araldite. Ultrathin sections were prepared with a microtome and mounted on copper grids. As the last step, samples were stained with 2% uranyl acetate and lead citrate. They were then observed in a transmission electron microscope (TEM; Jeol, Japan) and the number of autophagosomes was manually counted.

## 2.11. Tunel

Apoptosis in xenografts from mice in the oe-NC, oe-TRIM13, and oe-TRIM13+oe-NRF2 groups was assessed using a TUNEL Assay Kit-Alexa Fluor™ 488 (C10617, Invitrogen). Specimens ( $n = 5$ /group) were cut into 5  $\mu$ m sections, paraffin-embedded, hydrated with an ethanol gradient (100%, 95%, 85%, 70%, and 50%), fixed with 4% formaldehyde solution, and incubated with proteinase K for 20 min at room temperature. For each specimen, at least three slices were used. To block endogenous peroxidases, 3% hydrogen peroxide was used. TUNEL reaction solution was prepared temporarily according to the manufacturer's protocols. After washing with PBS, the slices were counterstained with DAPI for nuclear staining. Apoptotic signals were captured under five randomly selected fields with an OLYMPUS B×51 microscope and quantified with the ImageJ software.

## 2.12. DCFH-DA staining

DCFH-DA staining was used to evaluate the intracellular level of ROS. Briefly, A549 and HCC287 cells were incubated with 10  $\mu$ M DCFH-DA (Beyotime) under the manufacturer's guidance. Cells were incubated at 37°C for 30 min and subsequently washed 1 to 2 times with cell culture medium (serum-free). Intracellular ROS was observed via an OLYMPUS B×51-FL microscopy

(Olympus, Japan) and fluorescence intensity was quantified with the ImageJ software.

### 2.13. Immunofluorescence

Existence of LC3 and co-localization of TRIM13 and p62 were assessed using immunofluorescence. A549 and HCC287 cells were fixed with 4% paraformaldehyde and permeabilized with 0.2% Triton X-100. After washing with PBS, slides were blocked with 2% BSA in PBS for 1.5 h at room temperature, followed by overnight incubation with primary antibodies, anti-LC3 (1:500, cat. no. Ab192890), anti-TRIM13 (1:100, cat. no. Ab234847) and anti-p62 (1:50, sc-48,402).

The next day, cells were washed thrice with PBS and incubated with fluorochrome-conjugated secondary goat anti-rabbit antibody at room temperature for 1 h. Nuclei were stained with DAPI (Beyotime) at 0.1 g/mL for 5 min and images were analyzed via a confocal microscopy (Zeiss LSM 510 confocal). Immunofluorescence intensity was analyzed using the ImageJ software.

### 2.14. Co-immunoprecipitation (Co-IP)

A549, HCC827 cell lines were tagged with Flag-TRIM13 and HA-62. After 48 h, cells were harvested and lysed in lysis buffer (containing 1% NP-40, Jiangsu, China). The extracts were incubated with anti-Flag and HA antibodies at 4°C for 1 h with slow rotation. IP buffer was used five times to wash away unbound proteins. The immunoprecipitated products were visualized and measured using western blot.

### 2.15. Immunoprecipitation (IP)

A549 cell lysate was extracted on ice for 2 h, centrifuged, and incubated with antibody-conjugated beads at 4°C overnight. Antibody-bead complexes were washed 5 or 6 times with cold lysis buffer. SDS-PAGE loading buffer was utilized to release the precipitated proteins from the resins by boiling them for 15 min. The boiled immune complexes were placed on ice for 2 min and proceeded for SDS-PAGE electrophoresis.

### 2.16. Animal models

Animal experiments were conducted following institutional guidelines set forth by the ethics board. The female nude mice (5 wk, 18–20 g,  $n = 5$ /group) were injected subcutaneously (SC) with  $5 \times 10^5$  A549 cells transfected with oe-NC, oe-TRIM13, and oe-TRIM13+oe-NRF2 into the right flank of a nude mouse. Tumor growth was examined weekly for at least 4 wk. After 28 d, the mice were euthanized, and tumor volumes were calculated using the formula:  $V = (ab^2)/2$  where  $a =$  tumor length and  $b =$  tumor width.

### 2.17. Statistical analysis

Data were expressed as the mean  $\pm$  standard deviation of three independent assays. Statistical analysis was conducted using GraphPad Prism 7 software. Shapiro–Wilk test was performed to assess normality, and all data passed the normality test. Comparisons between two groups were assessed with two-tailed Student's  $t$ -test and comparisons among multiple groups were assessed with one-way ANOVA followed by Tukey's post hoc test. The five-year overall survival curve was generated by Kaplan-Meier Plotter online database [36]. Association of TRIM13 expression and clinicopathological parameters in LUAD was analyzed by the chi-square test. A  $p$ -value less than 0.05 ( $P < 0.05$ ) in our results indicates statistical significance.

## 3. Results

### 3.1. Downregulation of TRIM13 in LUAD tissues

The expression of TRIM13 in 20 cases of matched LUAD and noncancerous lung tissue samples was detected by RT-PCR and Western blot assays. As shown in Figure 1a, the average TRIM13 expression was significantly lower in LUAD tissues than in normal tissue ( $P < 0.001$ ). IHC analysis also demonstrated the down-regulation of the TRIM13 in LAUD tissues as compared to normal counterparts as well as the subcellular location of TRIM13 in both cytoplasm and nucleus in LUAD (Figure 1b). The association of TRIM13 expression and clinicopathological parameters in LUAD was analyzed. The results indicated that TRIM13

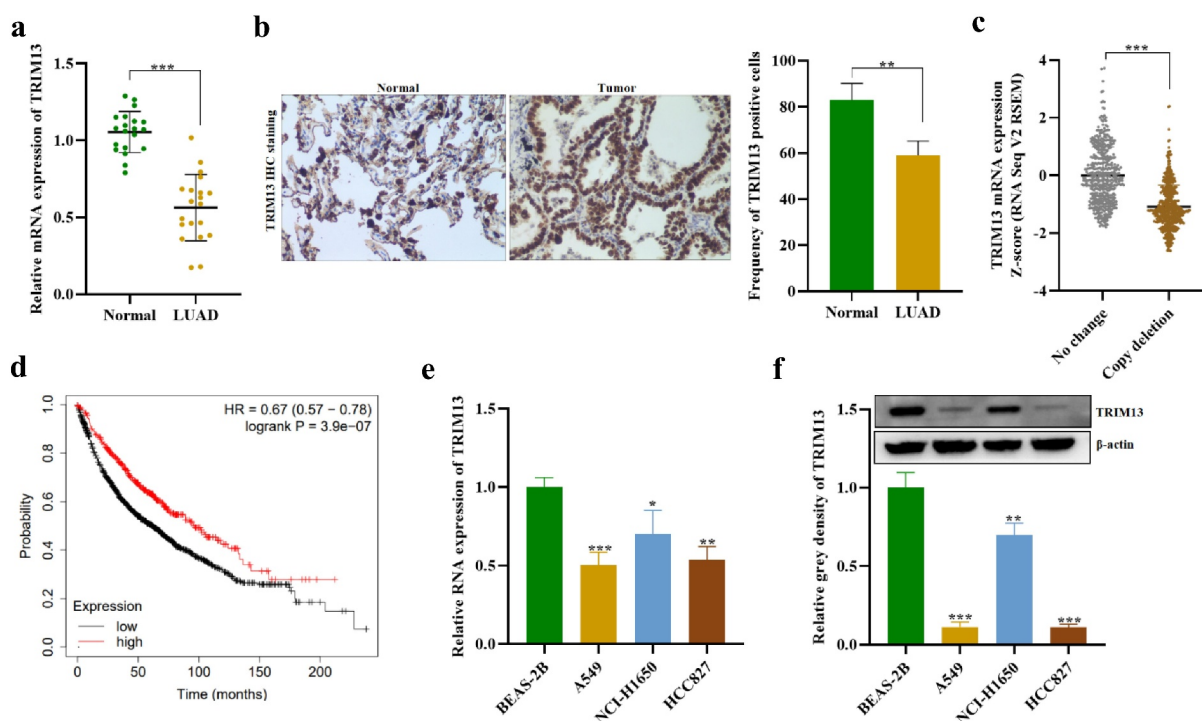


**Figure 1.** Downregulation of TRIM13 in LUAD tissues.

Note: (a-b) The levels of TRIM13 mRNA and protein were detected in LUAD tissue ( $n = 20$ ) and controls ( $n = 20$ ) using RT-qPCR and IHC, respectively, and were found to be lower in LUAD samples. (c) Analysis of cBioportal data revealed TRIM13 copy depletion in 652 out of 1249 LUAD samples. (d) Kaplan–Meier curve analysis showed that LUAD patients with low TRIM13 expression had reduced survival probability. (e-f) RT-qPCR and western blot analysis were performed to measure TRIM13 mRNA and protein levels in three LUAD cell lines (A549, NCI-H1650, and HCC827) and a control cell line (BEAS-2B), which demonstrated reduced expression in all LUAD cell lines, particularly in A549 and HCC827. Statistical analysis showed significant differences ( $*p < 0.05$ ,  $**p < 0.01$ ,  $***p < 0.001$ ).

**Table 1.** Association of TRIM13 expression and clinicopathological parameters in LUAD.

| Factors         | Sample size | TRIM13 high expression ( $n = 10$ ) | TRIM13 low expression ( $n = 10$ ) | P value  |
|-----------------|-------------|-------------------------------------|------------------------------------|----------|
| Age             |             |                                     |                                    | 0.3613   |
| <60             | 8           | 3                                   | 5                                  |          |
| $\geq 60$       | 12          | 7                                   | 5                                  |          |
| Gender          |             |                                     |                                    | 0.1596   |
| Male            | 13          | 5                                   | 8                                  |          |
| Female          | 7           | 5                                   | 2                                  |          |
| TNM stage       |             |                                     |                                    | 0.0617   |
| I               | 4           | 3                                   | 1                                  |          |
| II              | 9           | 6                                   | 3                                  |          |
| III+IV          | 7           | 1                                   | 6                                  |          |
| Pathology stage |             |                                     |                                    | 0.0074** |
| I               | 3           | 3                                   | 0                                  |          |
| II              | 11          | 7                                   | 4                                  |          |
| III             | 6           | 0                                   | 6                                  |          |
| Smoking         |             |                                     |                                    | 0.6531   |
| Yes             | 11          | 6                                   | 5                                  |          |
| No              | 9           | 4                                   | 5                                  |          |

Note:  $**p < 0.01$  indicates statistical significance.

expression had no association with age, gender, TNM stage, smoking, but had significant association with pathology stage (Table 1).

Bioinformatic analysis using cBioportal subset of Metastatic Non-Small Cell Lung Cancer,

Nature Medicine 2022 (<https://www.cbioportal.org/>) on 1249 LUAD samples also indicated reduced mRNA expression and copy deletion in 652 samples showing a correlation between TRIM3 copy deletion and mRNA expression

(Figure 1c). Kaplan–Meier curve showed that LAUD patients with low-level TRIM13 had a poor prognosis and reduced survival probability (Figure 1d). Finally, lower mRNA (Figure 1e) and protein (Figure 1f) of TRIM13 were observed in LAUD cell lines (A549, NCI-H1650, and HCC827) as compared to the control cell line (BEAS-2B). A549 and HCC827 showed relatively lower TRIM13 expression and will be used for experiments. Collectively, TRIM13 shows depletion in LAUD tissue and cells and indicates poor prognosis of LAUD patients.

### 3.2. TRIM13 suppresses LAUD cell proliferation and facilitates cell apoptosis

We have verified that the basal level of TRIM13 is low in LAUD cell lines. A549 and HCC827 cell lines were generated that ectopically overexpressed TRIM13 (hereafter referred to as oe-TRIM13-A549 and oe-TRIM13-HCC827), while oe-NC without TRIM13 expression was used as a control (oe-NC). TRIM13 expression in the transfected cells was detected by RT-PCR analysis (Figure 2a). Reverse transcription analysis revealed that expression of TRIM13 at mRNA level was increased in both LAUD cells compared with the control. The above result confirmed the expression of recombinant plasmids in transfected cells with TRIM13, indicating that the exogenous TRIM13 was successfully transfected into the LAUD cells.

TRIM proteins belong to the RNF protein family that contains the N-terminal RING domain. TRIM13 performs its biological functions using the RING finger domain [37]. Thus, we constructed plasmids of TRIM13 with a mutated RING finger domain (hereafter referred to as TRIM13- $\Delta$ RING). The relative proportion of TRIM13 protein in A549 and HCC827 cell lines transfected with wild-type oe-TRIM13 or TRIM13- $\Delta$ RING was examined. Interestingly, the mutation in RING finger domain of TRIM13 reduced TRIM13 expression in both cell lines, demonstrating that the TRIM13 RING domain depletion vector is successfully constructed (Figure 2b).

To test whether TRIM13 may function as a tumor suppressor, a clonogenic assay was performed to analyze the effect of TRIM13

upregulation on *in vitro* growth of LAUD cell lines. Compared with oe-NC and TRIM13- $\Delta$ RING, the colony number decreased by oe-TRIM13 by about 50% ( $p < 0.001$ ) in both cell lines (Figure 2c). To further testify an antiproliferative effect of TRIM13 on the viability of LAUD cells, CCK8 assay was performed. As shown in Figure 2d, oe-TRIM13-A549 and oe-TRIM13-HCC827 cells grew more slowly than oe-NC and oe-TRIM13- $\Delta$ RING cells.

To understand if apoptosis was associated with growth restriction, we performed flow cytometry to analyze the apoptosis of LAUD cells with or without the exogenous TRIM13 gene and its mutated version. Annexin V FITC/PI staining of cells was analyzed by flow cytometry, and a substantial increase in the level of apoptotic cells was detected (Figure 2e). Moreover, western blot was conducted to assess apoptosis-associated proteins (Bax and Bcl-2) and cyclins (Cyclin A1 and Cyclin D1). oe-TRIM13-A549 and oe-TRIM13-HCC827 cells showed a significant increase in Bax protein level and a significant increase in Bcl-2, Cyclin A1, and Cyclin D1 protein levels (Figure 2f). Taken together, these results suggest that ectopic expression of TRIM13 can trigger apoptosis in LAUD cells, which was dependent on the RING domain.

### 3.3. TRIM13 facilitates LAUD cell autophagy and oxidative stress

The above data demonstrated that TRIM13 facilitates the induction of apoptosis in LAUD cells, it was unclear whether autophagy was activated. Therefore, to investigate its involvement, we first assessed the level of autophagy in LAUD cell lines. We characterized it using two classical assays: (1) TEM analysis of the cytoplasmic accumulation of autophagosomes, a direct way to detect autophagy activation, and immunofluorescence staining of LC3, an autophagy-specific marker. TEM Images (Figure 3a) showed marked elevation of autophagosome number in A549 and HCC827 cells overexpressed with TRIM13. However, mutation of the RING domain in TRIM13 resulted in a significantly decreased number of the autophagosomes compared with the wild-type oe-TRIM13 group. To further corroborate that TRIM13

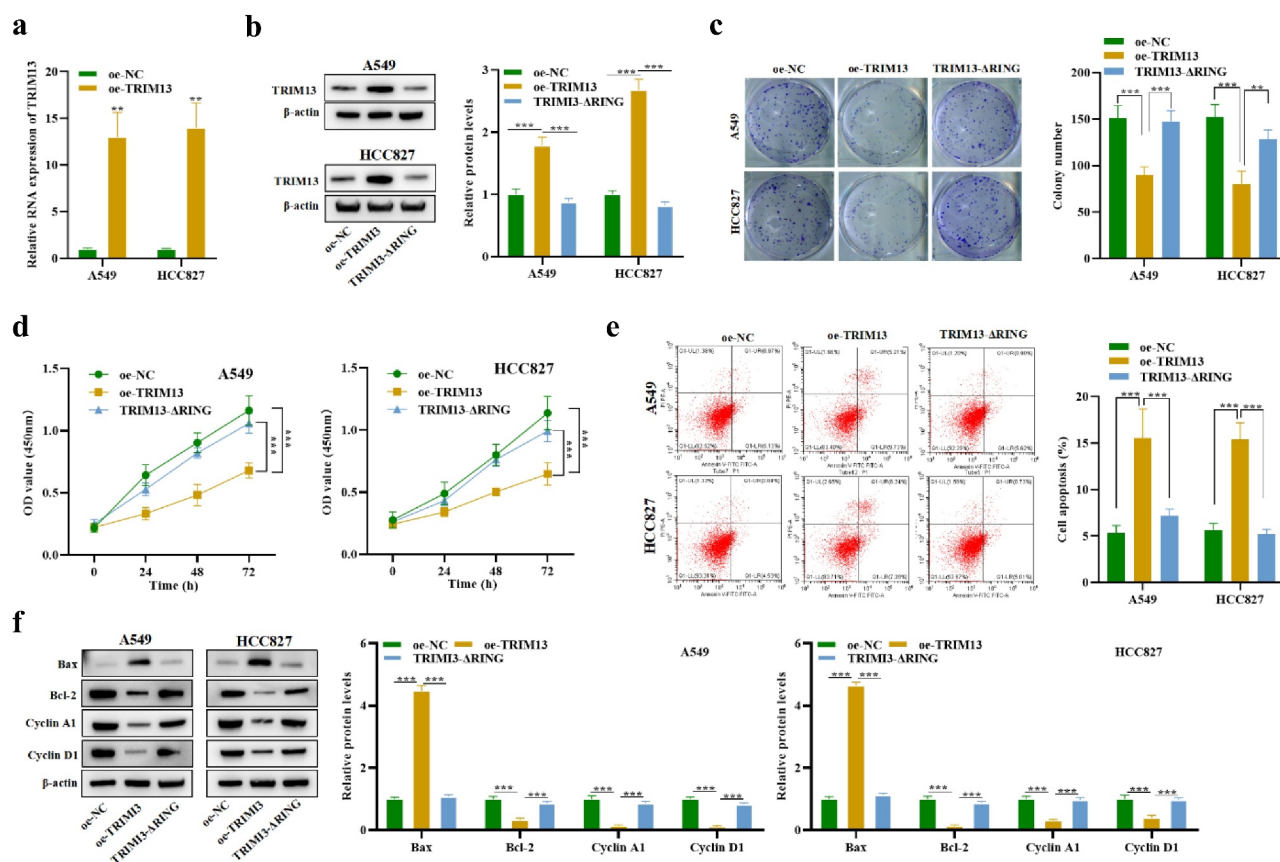


**Figure 2.** Ectopic expression of TRIM13 suppressed LUAD cells proliferation and facilitated cell apoptosis. LUAD cells were transfected with TRIM13 and its mutated version.

Note: (a) The mRNA expression of TRIM13 in A549 and HCC827 cell lines was detected using RT-qPCR after transfection with oe-TRIM13 and its mutated version and compared with control cells. (b) The transfection efficacy of oe-TRIM13 and oe-TRIM13-ΔRING was detected in LUAD cells using western blot analysis. (c) Colony formation assay showed reduced growth in LUAD cells transfected with oe-TRIM13 as compared to control and mutated version. (d) CCK-8 assay was performed to evaluate LUAD cell viability and proliferation by measuring OD absorbance. Results showed that oe-TRIM13-A549 and oe-TRIM13-HCC827 cells grew more slowly than oe-NC and oe-TRIM13-ΔRING cells. (e) TRIM13 expression increased apoptosis in LUAD cells. The apoptotic rate of transfected cells was determined using flow cytometry. (f) The protein levels of Bax, Bcl-2, Cyclin A1, and Cyclin D1 in LUAD cells transfected with oe-TRIM13 and oe-TRIM13-ΔRING were detected using western blot analysis. The data represents the mean  $\pm$  S.D. from three independent experiments, and statistical significance was determined using ANOVA test with \*\*  $P < 0.01$  and \*\*\* $P < 0.001$ .

influences the autophagosome formation, we directly assessed LC3 expression using immunofluorescence.

Notably, TRIM13 overexpression dramatically increased LC3 expression in A549, HCC827 cells, whereas mutation in the RING domain significantly decreased the percentage of LC3 positive cells compared with the oe-TRIM13 group (Figure 3b), further proving that TRIM13 affects the autophagy process. Together, our results indicate that TRIM13 is associated with increased autophagosome formation and autophagy, and it requires the cooperation of the RING finger domain. Several reports indicated the contribution of reactive oxygen species (ROS) in the induction

of autophagy and apoptosis [38,39]. Therefore, we decided to analyze the concentration of ROS accumulation in the cells. For this purpose, cells were stained with CM-H2-DCFH-DA, a fluorescence dye that reacts to a broad spectrum of ROS. The fluorescence intensity was analyzed using the ImageJ software. As shown in Figure 3c, ROS level was increased significantly by overexpression of TRIM13 in A549 and HCC827 cells. Interestingly, this increased ROS generation was efficiently attenuated in the presence of a mutated RING domain. Collectively, TRIM13 promotes the induction of autophagy and oxidative stress in lung cancer cells through the involvement of the RING finger domain.



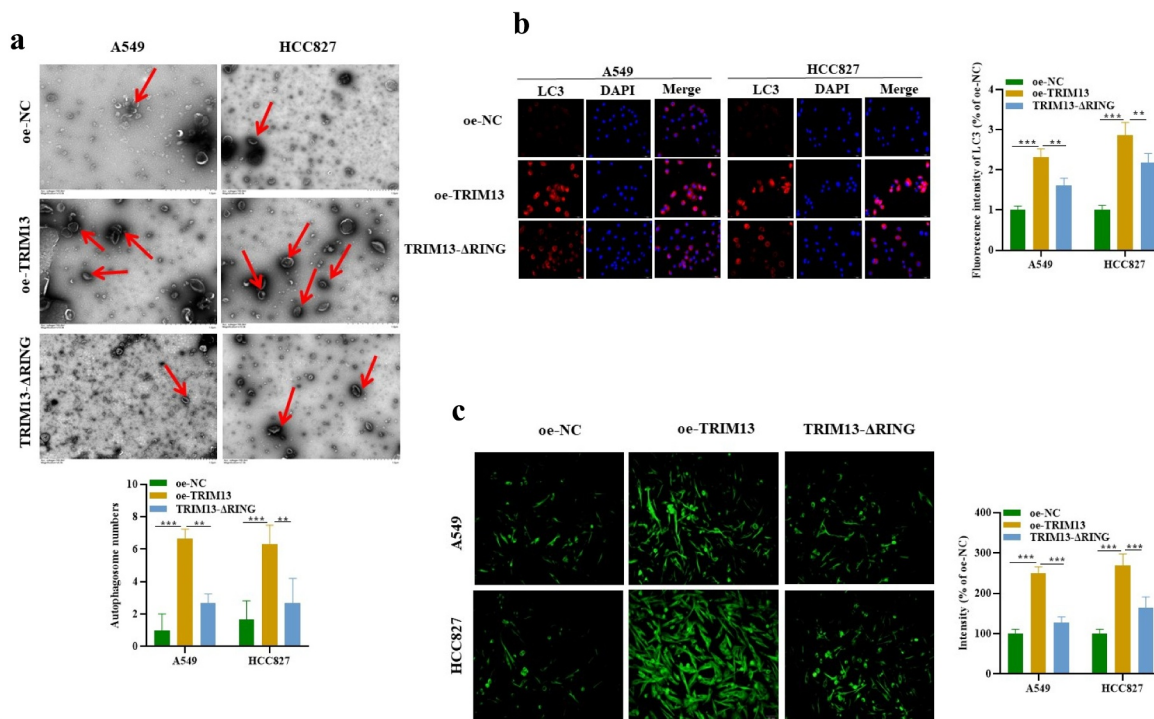


**Figure 3.** TRIM13 facilitated LUAD cell autophagy and oxidative stress.

Note: TEM images were captured, and autophagosomes in oe-NC, oe-TRIM13, or oe-TRIM13-ΔRING group were counted manually. Autophagosomes, marked by red arrows, were significantly elevated in TRIM13-overexpressing A549 and HCC827 cells. (a) LC3 immunofluorescence staining was used to detect LUAD cell autophagy. TRIM13 overexpression significantly increased autophagy in A549 and HCC827 cells as compared to the control and LUAD cells with the mutated version of TRIM13. (c) DCFH-DA staining was used to detect oxidative stress in all constructs. ROS levels were significantly increased in the LUAD cells expressing TRIM13. Significance was set at \*\*  $P < 0.01$  and \*\*\* $P < 0.001$ .

### 3.4. TRIM13 interacts with p62 protein in LUAD cells

Next, we explored the downstream gene of TRIM13 regulating the LUAD cell malignant behaviors. String and BioGrid databases were searched for protein-protein interaction (PPI) of TRIM13. Interestingly, autophagy-related marker p62 (SQSTM1) showed a strong correlation with TRIM13 in both databases (Figure 4a) which were further validated with RT-qPCR and western blot. Results showed the reduced protein level of p62 in TRIM13 overexpressed cells. However, this effect was only observed at the protein level and mRNA level of p62 was not influenced (Figure 4b). Finally, TRIM13 co-localized with p62 in the cytoplasm (Figure 4c), and oe-TRIM13 decreased p62 expression in LUAD cells, suggesting that TRIM13 regulates p62 at a post-transcriptional level.

Finally, fusion proteins Flag-TRIM13 and HA-p62 were constructed to validate the interaction of both proteins using Co-IP. The results confirmed

that both Flag-TRIM13 and HA-p62 in A549 and HCC827 cells were co-immunoprecipitated with anti-Flag or anti-HA rather than IgG (Figure 4d). Taken together, TRIM13 has been shown to interact with p62 in LUAD cells.

### 3.5. TRIM13 mediates p62 ubiquitination in LUAD cells

Ubiquitination is a post-transcriptional modification, where ubiquitin moiety is covalently attached to the substrate protein and indicates autophagic degradation. TRIM13 is an E3 ligase and mediates the protein ubiquitination, whereas p62 is an autophagy substrate. Findings from our previous results demonstrate that TRIM13 suppresses p62 protein expression, we speculated that TRIM13 may mediate the process via p62 ubiquitination. Western blot results indicated that the inhibitory effect of TRIM13 on protein p62 in A549 cells was abrogated by the addition of 10 mM of a protease

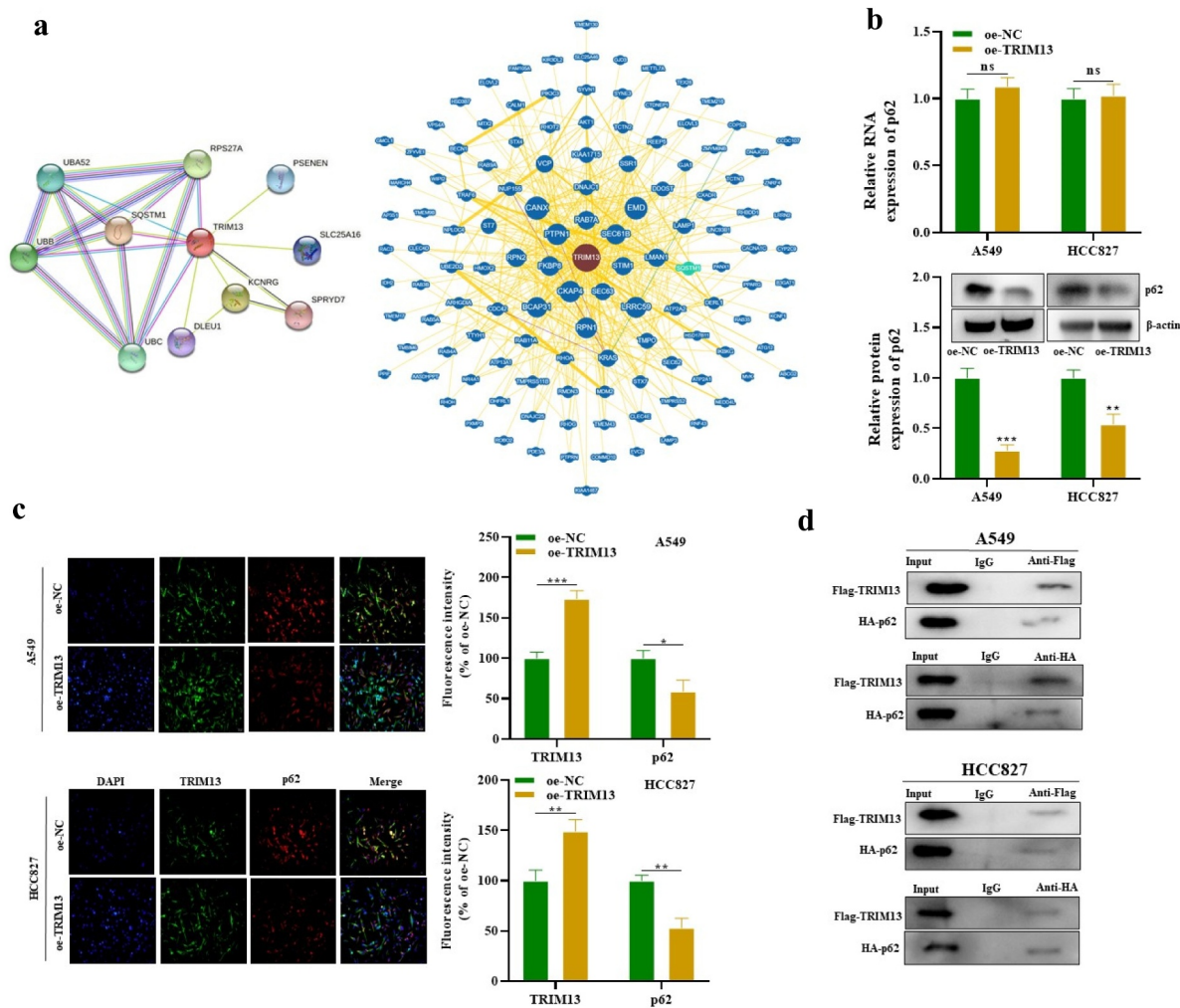


**Figure 4.** TRIM13 interacts with p62 protein in LUAD cells.

Note: (a) The PPI network of TRIM13 was predicted using String and BioGrid databases. Autophagy-related marker p62 (SQSTM1) showed a strong correlation with TRIM13. (b) The protein level of p62 was significantly reduced in oe-TRIM13-transfected LUAD cells compared to oe-NC, but no significant change was observed at the mRNA level as measured by RT-qPCR (upper graph) and western blot (lower graph). (c) Co-localization of P62 with TRIM13 in oe-NC- or oe-TRIM13-transfected LUAD cells was detected by immunofluorescence. (d) Co-IP experiments detected the interaction between P62 and TRIM13 in Flag-TRIM13- or HA-p62-transfected LUAD cells. \*  $P < 0.05$ , \*\*  $P < 0.01$ , \*\*\* $P < 0.001$  were considered significant values, while “ns” indicates no significance.

inhibitor, MG132 (Figure 5a) confirming that TRIM13 degrades p62 protein. We next treated oe-TRIM13-A549 cells and oe-NC-A549 cells by CHX for the indicated time (4,6,8 h) to examine protein abundance. CHX caused a gradual and time-dependent decline of the p62 protein level. The oe-TRIM13-A549 cells had a more significant decline of p62 protein level than the oe-NC-A549 cells, indicating the role of TRIM13 in degrading the p62 protein (Figure 5b). Finally, IP and WB further confirmed the ubiquitination and decreased protein level of p62 in oe-TRIM13-A549 cells (Figure 5c). These data suggest that

p62 is targeted by TRIM13 for ubiquitination in LUAD cells.

### 3.6. TRIM13 regulates the Keap1/Nrf2 pathway in LUAD cells

The Keap1-Nrf2 pathway is the primary protective action of the cell against oxidative stress. Under normal circumstances, Keap1, a vital part of an E3 ubiquitin ligase, targets NRF2 for proteasome-dependent degradation [40]. However, in stress, Keap1 allows Nrf2 to escape ubiquitination and translocate to the nucleus,

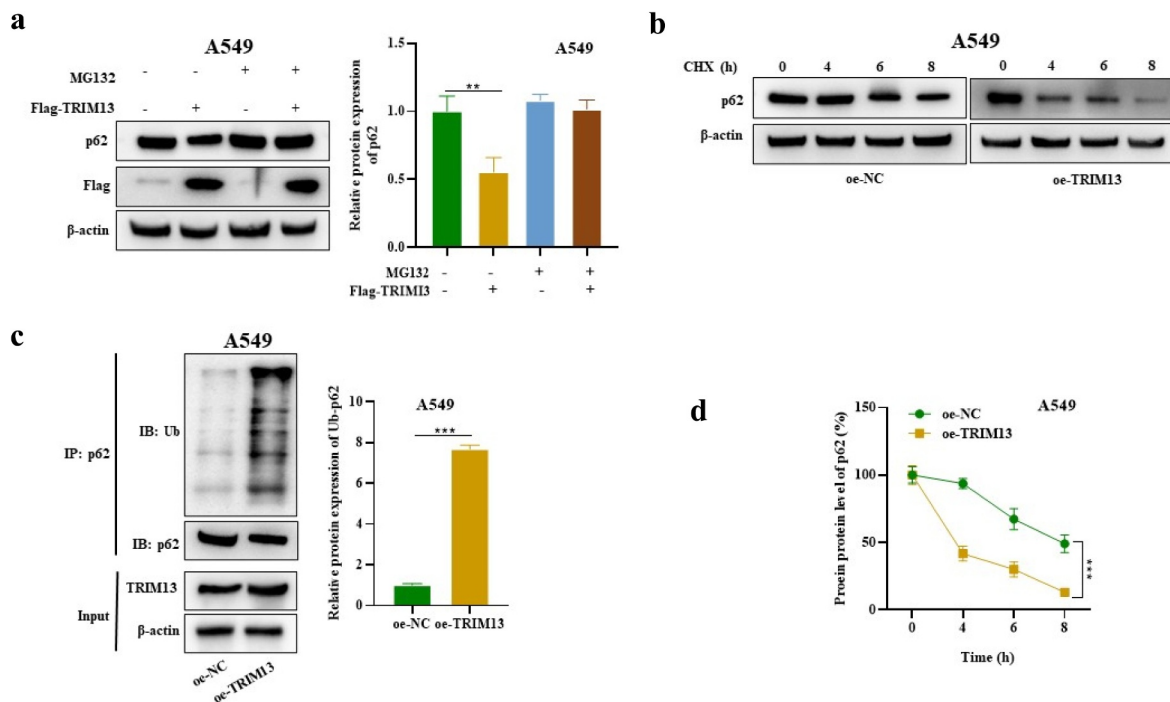


**Figure 5.** TRIM13 mediated SQSTM1 ubiquitination in LUAD cells.

Note: (a) The p62 level in MG132± and Flag-TRIM13± A549 cells was measured by Western blot. (b) The p62 protein level was measured by Western blot in oe-NC- or oe-TRIM13-transfected A549 cells with CHX treatment at different time points. A gradual and time-dependent decline of the p62 protein level in oe-TRIM13-A549 cells indicates the involvement of TRIM13 in p62 protein degradation. (c) IP-WB was used to detect the p62 ubiquitination level in oe-NC- or oe-TRIM13-transfected A549 cells. \*\* P < 0.01, \*\*\*P < 0.001 indicate significant values. (d) The reduced p62 protein level in oe-TRIM13-A549 cells suggests that TRIM13 targets p62 for ubiquitination in LUAD cells.

where it can initiate its antioxidant mechanism. To explore whether TRIM13 regulates the Nrf2/Keap1 pathway, the cytoplasmic level of Keap1, whereas the cytoplasmic and nuclear levels of Nrf2 were measured in A549 and HCC827 cells. The western blot result showed that TRIM13 overexpression in these LAUD cells increased cytosolic Keap1 whereas reduced the cytoplasmic and nuclear expression of Nrf2, indicating the inactivation of the Nrf2 pathway (Figure 6a). Nrf2 is a transcriptional regulator of cellular antioxidant genes. Therefore, the mRNA level of downstream antioxidant enzymes, HO-1 and NQO1, was measured in LUAD cells. Accordingly, the mRNA levels of antioxidant HMOX1 and NQO1 were much lower in A549 and HCC827 cells overexpressed with TRIM13 (Figure 6b). The collective results indicate that TRIM13 exerts tumor suppressor functions in lung cancer cells by negatively regulating Nrf2 signaling and downstream antioxidants.

### 3.7. TRIM13 regulates LUAD cell malignancy through Nrf2

Next, A549 cells were transfected with Nrf2 overexpression vector (oe-NRF2) to investigate whether Nrf2 regulates the functions of LUAD cells. Figure 7a shows successful transfection in these cells by RT-PCR. Interestingly, oe-Nrf2 increased cell proliferation (Figure 7b), enhanced cell viability (Figure 7c), and reduced apoptotic rate (Figure 7d–e), autophagosome number (Figure 7f), LC3 expression (Figure 7g) and oxidative stress (Figure 7h) thus countering the effects of TRIM13 to some extent (Figure 7b–h). It suggests that TRIM13 suppresses LUAD cell malignancy through controlling NRF2.

### 3.8. TRIM13 suppresses LUAD tumor growth through NRF2 *in vivo*

Based on *in vitro* data, we sought to determine whether TRIM13 exerts an antitumor effect via

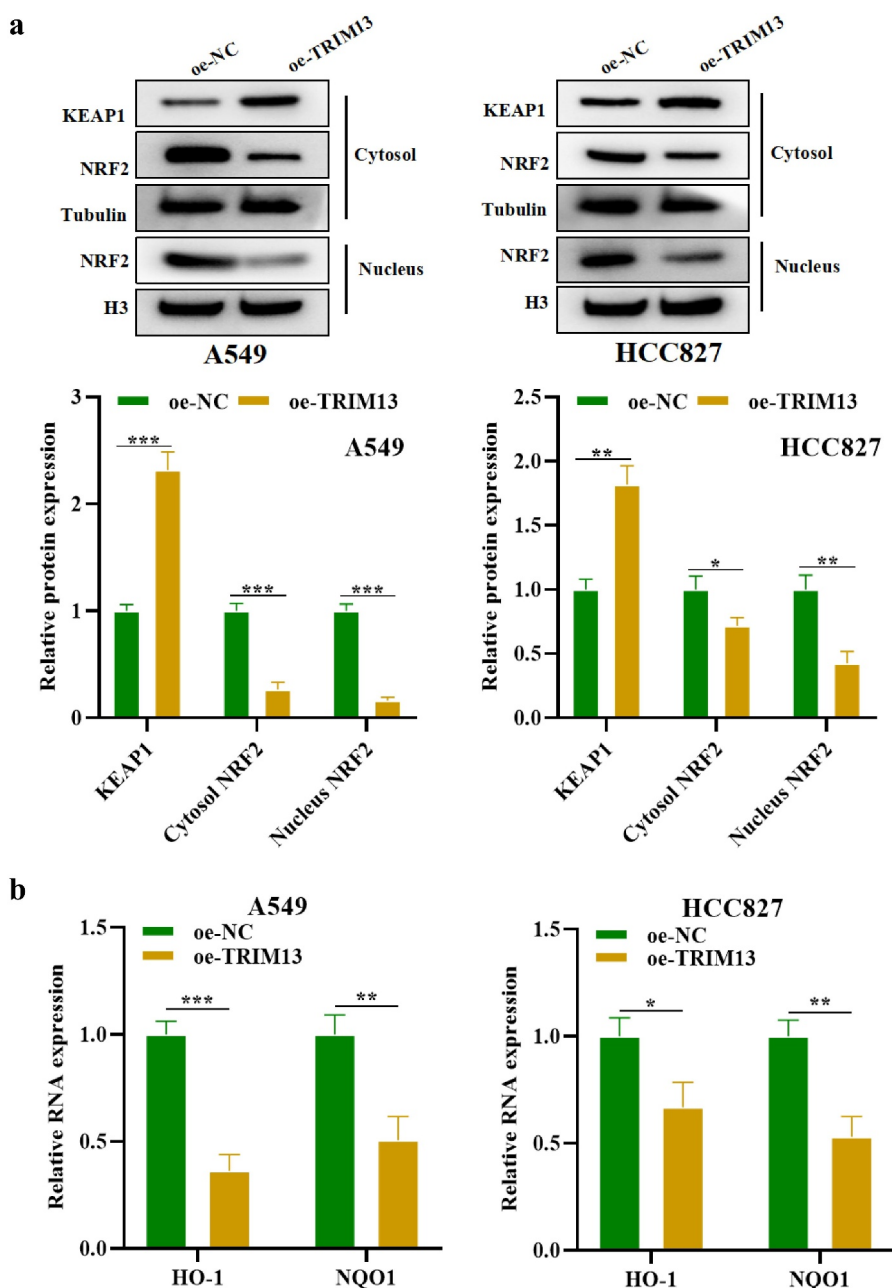


**Figure 6.** TRIM13 regulates the Keap1/Nrf2 pathway in LUAD cells.

Note: (a) Western blot analysis was performed to determine the protein levels of Keap1/Nrf2 pathway-related proteins in LUAD cells transfected with oe-NC or oe-TRIM13. Results showed that TRIM13 overexpression increased Keap1 protein levels while reducing both cytoplasmic and nuclear Nrf2 expression, indicating inactivation of the Nrf2 pathway. (b) RT-qPCR analysis demonstrated that the mRNA levels of downstream antioxidant enzymes of Nrf2, such as HO-1 and NQO1, were significantly lower in oe-TRIM13-transfected LUAD cells compared to control cells. The statistical significance was set at \*  $P < 0.05$ , \*\*  $P < 0.01$ , and \*\*\* $P < 0.001$ .

Nrf2 *in vivo*.  $5 \times 10^5$  A549 cells expressing oe-NC, oe-TRIM13, and oe-TRIM13+oe-Nrf2 were subcutaneously injected into the flank of nude mice. Tumor volume was monitored for 28 d. Mice were killed after 28 d of implantation, and xenografts were weighed. The results revealed that injecting oe-TRIM13-A549 cells reduced the

tumor volume, size, and weight in the xenografts. Interestingly, tumor volume, size, and weight from xenograft established by injecting the oe-TRIM13-oe-NRF2-A549 cells were bigger than oe-TRIM13-A549 tumors (Figure 8a, b). IHC analysis revealed a significant decrease in Ki67 (proliferation marker) in xenograft sections from oe-TRIM13-A549

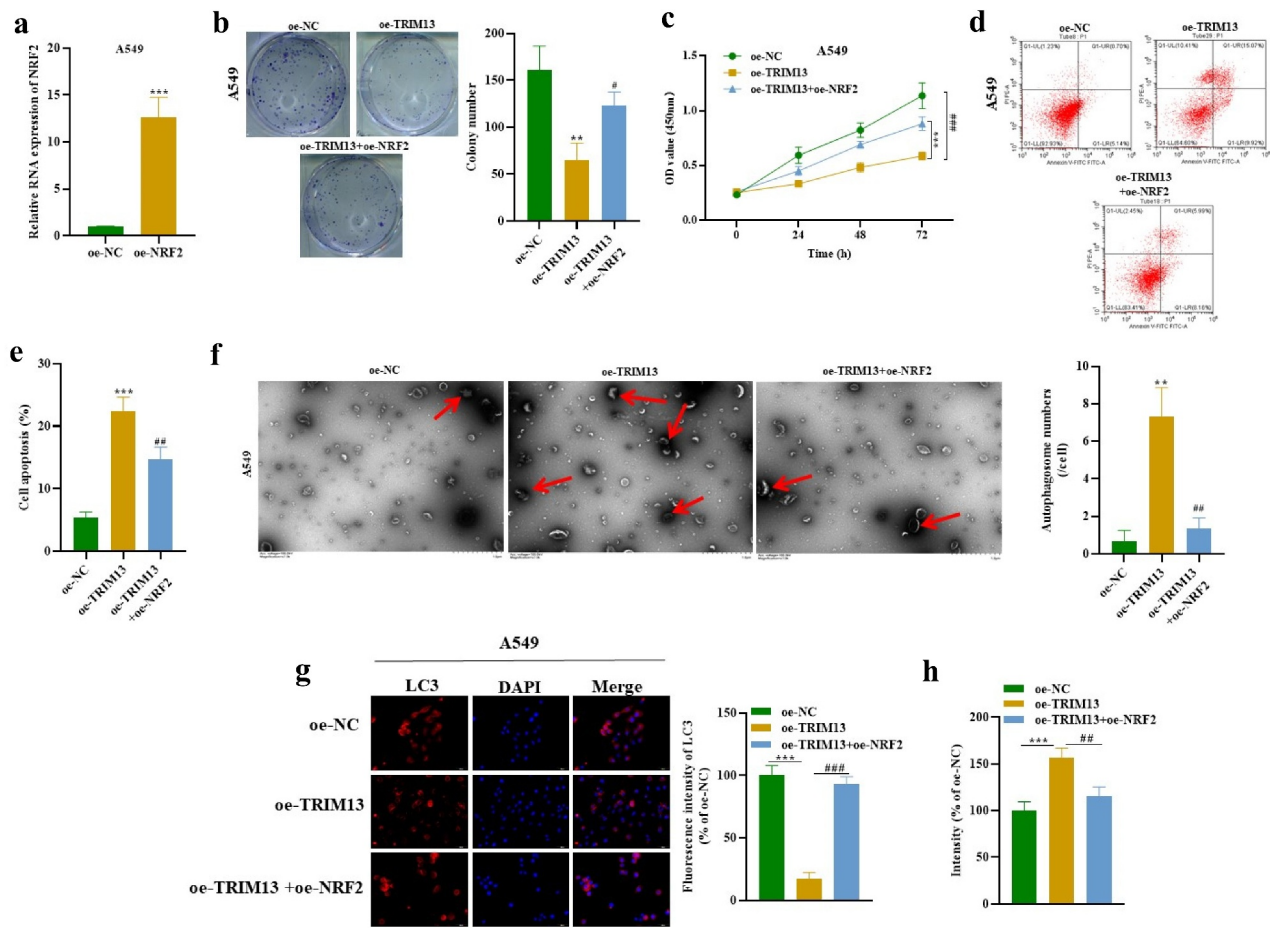


**Figure 7.** TRIM13 regulated LUAD cell malignancy through NRF2.

Note: (a) The transfection efficacy of oe-NRF2 in A549 cells was determined by RT-qPCR. (b) Colony formation assay revealed reduced LUAD cell proliferation in oe-TRIM13 group compared to oe-NC or oe-TRIM13+oe-Nrf2 group. (c) Cell viability was assessed by CCK-8 in all constructs. (d-e) Flow cytometry analysis demonstrated reduced LUAD cell apoptosis following Nrf2 transfection. (f) TEM images were captured, and autophagosomes in LUAD cells (marked by red arrows) were counted in each construct. NRF2 expression resulted in a decrease in the autophagosome level in A549 LUAD cells, partially reversing the effects of TRIM13. (g) LC3 staining was performed to detect LUAD cell autophagy. (h) DCFH-DA staining was used to measure LUAD cell oxidative stress. \*\* $P < 0.01$ , \*\*\* $P < 0.001$  and # $P < 0.05$ , ## $P < 0.01$ , ### $P < 0.001$  were considered significant.

group when compared to sections from oe-TRIM13+oe-Nrf2 and the control group (Figure 8c, d). This suggests that TRIM13 is a tumor suppressor and controls excessive cell proliferation. Ki67 data from Oe-TRIM13+oe-Nrf2 xenograft tissue sections revealed that cells can proliferate at a higher rate in the presence of Nrf2, but this proliferation was controlled by TRIM13 and thus proliferation was lower than the control group. Moreover, there was a significant increase in TUNEL positive cells and a significant decrease in p62 positive cells in xenograft sections from oe-TRIM13-A549 group when compared to sections from oe-TRIM13+oe-Nrf2 and the control group (Figure 8e, f). These

findings revealed that TRIM13 induces apoptosis and autophagy *in vivo* dependent on Nrf2 depletion.

These findings provide compelling evidence that TRIM13 overexpression reduces tumor development in the xenograft mice model. Altogether, these results provide the first *in vivo* evidence that TRIM13 negatively regulates tumor growth in mice models via Nrf2 downregulation and provides a novel insight for seeking targeted therapy of LUAD.

#### 4. Discussion

Though multiple treatment strategies and diagnostic techniques have been developed for LC, the

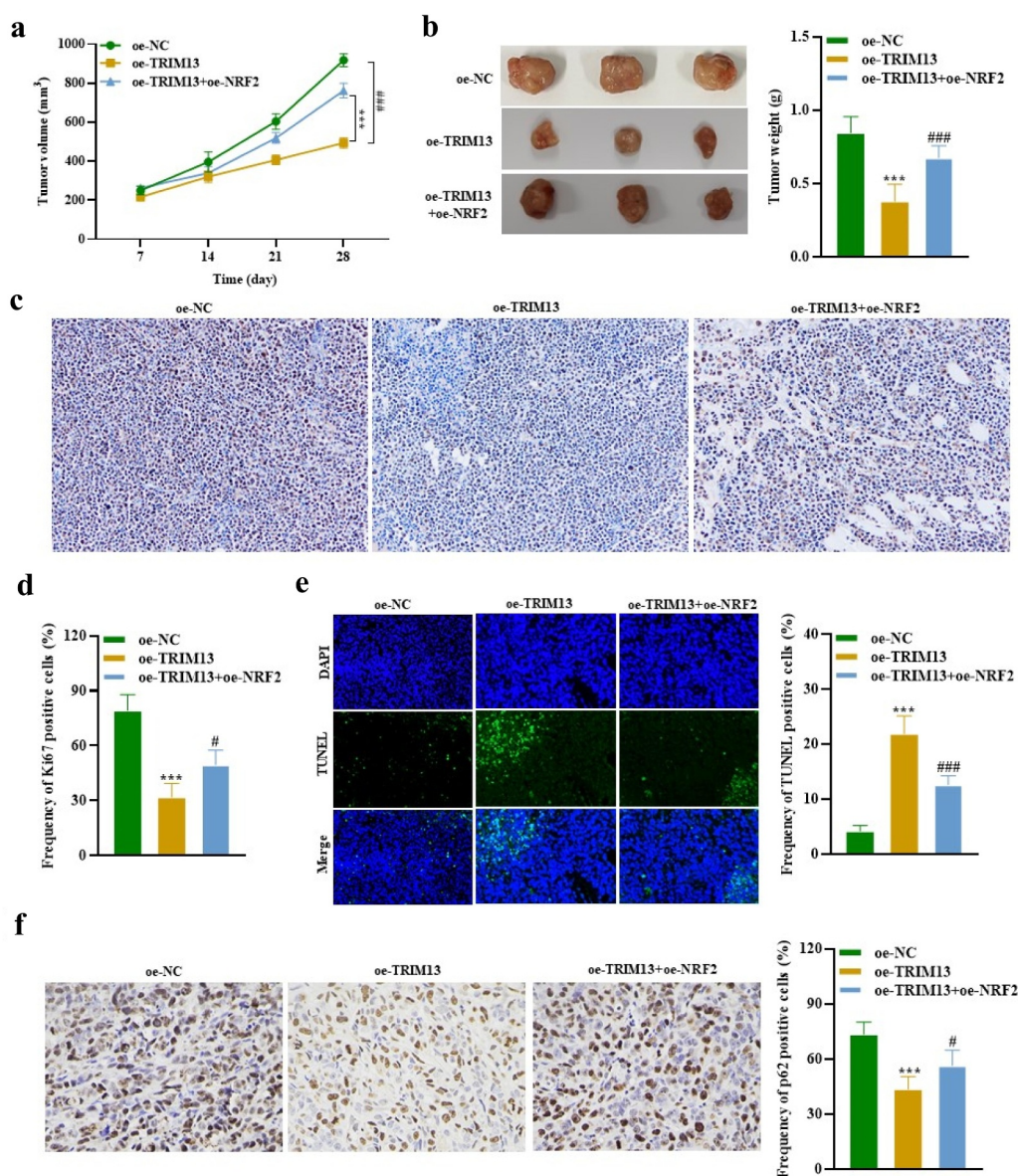


**Figure 8.** TRIM13 suppressed LUAD tumor growth through NRF2 in vivo.

Note: (a) Xenografts injected with TRIM13-overexpressing A549 cells showed a significant reduction in tumor volume. (b) Tumors derived from TRIM13-overexpressing A549 cells exhibited reduced weight in each mouse, whereas the presence of NRF2 increased the tumor weight. The images of tumors in panel B illustrate the reduced tumor size due to TRIM13 overexpression. (c) Immunohistochemical analysis of Ki67 expression in mouse xenograft tissues showed reduced tumor cell proliferation due to TRIM13 overexpression, as revealed by quantitative results presented in the graph (d). In E illustration, TUNEL staining of mouse xenografts and corresponding quantitative data indicated an increase in apoptotic events in the presence of TRIM13, which were reduced by NRF2. (f) IHC of p62 staining in mouse xenografts and corresponding quantitative data revealed a significant reduction in p62-positive cells in the presence of TRIM13, which was reversed by NRF2. Statistical significance was denoted by \*\*\* $P < 0.001$ , # $P < 0.05$ , and ### $P < 0.001$ .

survival rate of LC remains low, causing great distress to the physical and mental health of patients. Thus, it is of great significance to investigate the mechanism behind LC progression to develop appropriate therapeutic targets.

TRIM13 is an important member of the TRIM family and plays a diverse role in cell death [29] and endoplasmic reticulum-associated degradation [31]. It facilitates apoptosis via protein kinase B [29] and regulates autophagy in endoplasmic

reticulum stress [26]. Further studies have shown that Trim13 ubiquitinates Akt, L-type channels, and caspase-8 [41–43]. Bioinformatics analysis revealed lower *TRIM13* expression in breast cancer. TRIM13 has been shown to inhibit cell migration and invasion in renal cell carcinoma cell lines of 786-O [42]. A recent report showed that TRIM13 is downregulated in NSCLC cells and regulates NF- $\kappa$ B signaling in these cells [33]. These studies suggest the tumor suppressor function of TRIM13. Here, we found the reduced expression of TRIM13 in human LUAD tissues as compared to non-cancerous tissues, which is further confirmed by cBioportal data analysis. Additionally, TRIM13 overexpression in LUAD cell lines hampered cell proliferation and stimulated apoptosis in LUAD cells. However, this effect is reversed by a mutation in the RING domain of TRIM13 suggesting that tumor suppressor activity of TRIM13 depends on its RING finger domain.

Autophagy is a cellular protective mechanism against pathological conditions like infection, cancer, etc. [26]. The relationship between autophagy and apoptosis is controversial and highly dependent on the context. In some circumstances, autophagy counteracts apoptosis, whereas in other situations, autophagy acts synergistically with apoptosis [44]. Previous studies suggested that TRIM13 regulates autophagy and oxidative stress [45]. Autophagy has been closely associated with ROS [46,47]. ROS has been copiously reported as early inducers of autophagy upon nutrient deprivation [48].

In the present study, we found activation of autophagy and enhanced ROS accumulation in LUAD cells overexpressed with TRIM13, suggesting TRIM13 facilitated activation of autophagy and enhanced the oxidative stress in these cells. Ubiquitination plays an important role in the degradation of proteins or defective organelle either through proteasome or autophagy [26]. Different autophagy receptors interact with autophagy machinery [49]. p62 is a best-studied autophagy marker that can interact with ubiquitinated cargo [50]. This interaction leads to the degradation of the p62 level, which is associated with the activated autophagy process. LC3 is also often employed as a surrogate marker for autophagic vesicles [51].

Our study indicates a strong correlation of TRIM13 with p62 using String and BioGrid pathway, which was further validated experimentally. Interestingly, TRIM13 overexpression reduces the p62 level only at the protein level but not the mRNA value, indicating that TRIM13 degrades p62. We also found increased staining of LC3 in TRIM13-overexpressed LUAD cells suggesting autophagy activation in these cancer cells. This reduced protein level of an autophagy substrate, p62 in oe-TRIM13-A549 cells is caused by ubiquitination of TRIM13-mediated ubiquitination of p62, which was reversed by protease inhibitor, MG132. The RING finger domain can bind to ubiquitinase and substrate simultaneously and mediate ubiquitination. We demonstrated that ubiquitination of p62 by TRIM13 in LUAD cells takes place through its RING finger domain.

p62 is involved in multiple signal transduction pathways, including the Keap1–Nrf2 pathway [52]. It is a major signaling pathway that responds to increased oxidative stress [53]. Keap1 normally functions as an adaptor protein for the E3 ubiquitin ligase complex and sequesters Nrf2 in the cytoplasm at a low level [54]. Genomic data of humans have demonstrated that deregulation of this pathway is reported in multiple disorders. Mutations in Keap1–Nrf2 in lung cancer are associated with therapeutic resistance and poor prognosis [55]. Blake *et al.* showed malignant lung cancer in Keap1 Knock-out mice when exposed to additional proliferative stimuli [56]. Nrf2 inhibitors in advanced NSCLC patients harboring Keap1–Nrf2 mutation appear to be a promising treatment [57]. Substantial evidence has shown that p62 links autophagy to the Keap1–Nrf2 pathway [53,58].

In the p62–Keap1–Nrf2 interaction, the Keap1-interacting region of p62 binds to Keap1, thereby restricting Keap1 from trapping Nrf2. It results in stabilization and finally activation of Nrf2 [59]. The p62 gene is a target of Nrf2 [60], suggesting a positive-feedback loop within the p62–Keap1–Nrf2 axis. Autophagy is directly involved in the whole process. p62 is degraded by autophagy [61], and Keap1 is also degraded by autophagy in a p62 interaction manner [62]. We found the reduced cell apoptosis and increased cell proliferation and viability of LUAD cell line by transfection with oe-

Nrf2, suggesting that the negative impact of TRIM13 on tumor growth was through Nrf2 regulation. Accordingly, we found big tumors in xenografts injected with control cells, but with TRIM13 overexpression in these injected cells, the tumor remained smaller. Nrf2 in the presence of TRIM13 showed bigger tumors than TRIM13 overexpression ones, indicating that TRIM13 is a tumor suppressor and regresses tumor growth via the Nrf2 pathway.

In conclusion, TRIM13 triggers apoptosis and autophagy in LUAD cells through mediating p62 ubiquitination via KEAP1/NRF2 pathway, providing a novel insight for seeking targeted therapy for LUAD patients.

### Disclosure statement

No potential conflict of interest was reported by the authors.

### Funding

The author(s) reported that there is no funding associated with the work featured in this article.

### Authorship

Bo Yu and Yu Zhou planned, executed the experiments, and wrote the initial manuscript. Jinxi He performed statistical analysis. All authors revised the manuscript and approved for the final version.

### References

- [1] Siegel RL, Miller KD, Fuchs HE, et al. Cancer Statistics, 2021. *Ca A Cancer J Clinicians*. 2021;71(1):7–33.
- [2] Al-Dherasi A, Huang QT, Liao Y, et al. A seven-gene prognostic signature predicts overall survival of patients with lung adenocarcinoma (LUAD). *Cancer Cell Int*. 2021;21(1):294. Online First: Epub Date].
- [3] Ariozzi I, Paladini I, Gnetti L, et al. Computed tomography-histologic correlations in lung cancer. *Pathologica*. 2013;105(6):329–336.
- [4] Kozielski J, Kaczmarczyk G, Porębska I, et al. Lung cancer in patients under the age of 40 years. *Contemp Oncol (Pozn)*. 2012;16(5):413–415. Online First: Epub Date].
- [5] Cataldo VD, Gibbons DL, Pérez-Soler R, et al. Treatment of non-small-cell lung cancer with erlotinib or gefitinib. Online First: Epub Date]. *N Engl J Med*. 2011;364(10):947–955.

- [6] Bagherniya M, Butler AE, Barreto GE, et al. The effect of fasting or calorie restriction on autophagy induction: a review of the literature. *Ageing Res Rev*. 2018;47:183–197. Online First: Epub Date].
- [7] He L, Zhang J, Zhao J, et al. Autophagy: the Last Defense against Cellular Nutritional Stress. *Advances In Nutrition (Bethesda, MD)*. 2018;9(4):493–504. Online First: Epub Date].
- [8] Galluzzi L, Pietrocola F, Bravo-San Pedro JM, et al. Autophagy in malignant transformation and cancer progression. *Embo J*. 2015;34(7):856–880. Online First: Epub Date].
- [9] Tsujimoto Y, Shimizu S. Another way to die: autophagic programmed cell death. *Cell Death Diff*. 2005;12 Suppl 2(S2):1528–1534. Online First: Epub Date].
- [10] Liang J, Shao SH, Xu ZX, et al. The energy sensing LKB1-AMPK pathway regulates p27(kip1) phosphorylation mediating the decision to enter autophagy or apoptosis. *Nat Cell Biol*. 2007;9(2):218–224. Online First: Epub Date].
- [11] Degenhardt K, Mathew R, Beaudoin B, et al. Autophagy promotes tumor cell survival and restricts necrosis, inflammation, and tumorigenesis. *Cancer Cell*. 2006;10(1):51–64. Online First: Epub Date].
- [12] Li P, Du Q, Cao Z, et al. Interferon- $\gamma$  induces autophagy with growth inhibition and cell death in human hepatocellular carcinoma (HCC) cells through interferon-regulatory factor-1 (IRF-1). *Cancer Lett*. 2012;314(2):213–222. Online First: Epub Date].
- [13] Scherz-Shouval R, Shvets E, Fass E, et al. Reactive oxygen species are essential for autophagy and specifically regulate the activity of Atg4. Online First: Epub Date]. *Embo J*. 2007;26(7):1749–1760.
- [14] Seranova E, Connolly KJ, Zatyka M, et al. Dysregulation of autophagy as a common mechanism in lysosomal storage diseases. *Essays Biochem*. 2017;61(6):733–749. Online First: Epub Date].
- [15] Nixon RA. The role of autophagy in neurodegenerative disease. *Nature Med*. 2013;19(8):983–997. Online First: Epub Date].
- [16] Di Fazio P, Matrood S. Targeting autophagy in liver cancer. *Translational gastroenterology and hepatology*. 2018;3:39. Online First: Epub Date].
- [17] Qu X, Yu J, Bhagat G, et al. Promotion of tumorigenesis by heterozygous disruption of the beclin 1 autophagy gene. *J Clin Investig*. 2003;112(12):1809–1820. Online First: Epub Date].
- [18] Cicchini M, Chakrabarti R, Kongara S, et al. Autophagy regulator BECN1 suppresses mammary tumorigenesis driven by WNT1 activation and following parity. *Autophagy*. 2014;10(11):2036–2052. Online First: Epub Date].
- [19] Mathew R, Karp CM, Beaudoin B, et al. Autophagy suppresses tumorigenesis through elimination of p62. *Cell*. 2009;137(6):1062–1075. Online First: Epub Date].
- [20] Guo JY, Chen HY, Mathew R, et al. Activated Ras requires autophagy to maintain oxidative metabolism



- and tumorigenesis. *Genes Dev.* 2011;25(5):460–470. Online First: Epub Date].
- [21] Witz IP. Tumor-microenvironment interactions: dangerous liaisons. *Advances in cancer research.* 2008;100:203–229. Online First: Epub Date].
- [22] Yang L, Zhang X, Li H, et al. The long noncoding RNA HOTAIR activates autophagy by upregulating ATG3 and ATG7 in hepatocellular carcinoma. Online First: Epub Date] *Mol Biosyst.* 2016;12(8):2605–2612.
- [23] Lv D, Li Y, Zhang W, et al. TRIM24 is an oncogenic transcriptional co-activator of STAT3 in glioblastoma. *Nat Commun.* 2017;8(1):1454. Online First: Epub Date].
- [24] Czerwińska P, Mazurek S, Wiznerowicz M. The complexity of TRIM28 contribution to cancer. Online First: Epub Date] *J Biomed Sci.* 2017;24(1):63.
- [25] Cambiaghi V, Giuliani V, Lombardi S, et al. TRIM proteins in cancer. *Adv Exp Med Biol.* 2012;770:77–91. Online First: Epub Date].
- [26] Tomar D, Singh R, Singh AK, et al. TRIM13 regulates ER stress induced autophagy and clonogenic ability of the cells. Online First: Epub Date] *Biochim Biophys Acta.* 2012;1823(2):316–326.
- [27] Cheng B, Ren X, Kerppola TK. KAP1 represses differentiation-inducible genes in embryonic stem cells through cooperative binding with PRC1 and derepresses pluripotency-associated genes. Online First: Epub Date] *Mol Cell Biol.* 2014;34(11):2075–2091.
- [28] Oleksiewicz U, Gładych M, Raman AT, et al. TRIM28 and Interacting KRAB-ZNFs Control Self-Renewal of Human Pluripotent Stem Cells through Epigenetic Repression of Pro-differentiation Genes. *Stem Cell Rep.* 2017;9(6):2065–2080. Online First: Epub Date].
- [29] Joo HM, Kim JY, Jeong JB, et al. Ret finger protein 2 enhances ionizing radiation-induced apoptosis via degradation of AKT and MDM2. *Eur J Cell Biol.* 2011;90(5):420–431. Online First: Epub Date].
- [30] Tomar D, Singh R. TRIM13 regulates ubiquitination and turnover of NEMO to suppress TNF induced NF- $\kappa$ B activation. Online First: Epub Date] *Cell Signal.* 2014;26(12):2606–2613.
- [31] Lerner M, Corcoran M, Cepeda D, et al. The RBCC gene RFP2 (Leu5) encodes a novel transmembrane E3 ubiquitin ligase involved in ERAD. *Molecular biology of the cell.* Online First: Epub Date]. 2007;18(5):1670–1682.
- [32] Verfaillie T, Salazar M, Velasco G, et al. Linking ER Stress to Autophagy: potential Implications for Cancer Therapy. *Int J Cell Biol.* 2010;2010:930509. Online First: Epub Date].
- [33] Xu L, Wu Q, Zhou X, et al. TRIM13 inhibited cell proliferation and induced cell apoptosis by regulating NF- $\kappa$ B pathway in non-small-cell lung carcinoma cells. *Gene.* 2019;715:144015. Online First: Epub Date].
- [34] Tveden-Nyborg P, Bergmann TK, Jessen N, et al. BCPT policy for experimental and clinical studies. Online First: Epub Date] *Basic Clin Pharmacol Toxicol.* 2021;128(1):4–8.
- [35] Liu J, Zhang C, Xu D, et al. The ubiquitin ligase TRIM21 regulates mutant p53 accumulation and gain-of-function in cancer. *J Clin Investig.* 2023;133(6):Online First: Epub Date]. doi:10.1172/jci164354.
- [36] Györfy B. Survival analysis across the entire transcriptome identifies biomarkers with the highest prognostic power in breast cancer. *Comput Struct Biotechnol J.* 2021;19:4101–4109. Online First: Epub Date].
- [37] Cai C, Tang YD, Zhai J, et al. The RING finger protein family in health and disease. Signal transduction and targeted therapy. *Signal Transduct Target Ther.* 2022;7(1):300. Online First: Epub Date].
- [38] Macchioni L, Davidescu M, Sciacaluga M, et al. Mitochondrial dysfunction and effect of antiglycolytic bromopyruvic acid in GL15 glioblastoma cells. *J Bioenerg Biomembr.* 2011;43(5):507–518. Online First: Epub Date].
- [39] Kaminsky VO, Piskunova T, Zborovskaya IB, et al. Suppression of basal autophagy reduces lung cancer cell proliferation and enhances caspase-dependent and -independent apoptosis by stimulating ROS formation. Online First: Epub Date] *Autophagy.* 2012;8(7):1032–1044.
- [40] Baird L, Yamamoto M. The Molecular Mechanisms Regulating the KEAP1-NRF2 Pathway. *Mol Cell Biol.* 2020;40(13):Online First: Epub Date]. DOI:10.1128/MCB.00099-20.
- [41] Tan P, He L, Cui J, et al. Assembly of the WHIP-TRIM14-PPP6C Mitochondrial Complex Promotes RIG-I-Mediated Antiviral Signaling. *Molecular Cell.* 2017;68(2):293–307.e5. Online First: Epub Date].
- [42] Yang B, Wang J, Wang Y, et al. Novel function of Trim44 promotes an antiviral response by stabilizing VISA. *J Immun (Baltimore, Md. : 1950)* Online First: Epub Date].
- [43] Castanier C, Zemirli N, Portier A, et al. MAVS ubiquitination by the E3 ligase TRIM25 and degradation by the proteasome is involved in type I interferon production after activation of the antiviral RIG-I-like receptors. *BMC Biol.* 2012;10:44. Online First: Epub Date].
- [44] Liu G, Pei F, Yang F, et al. Role of Autophagy and Apoptosis in Non-Small-Cell Lung Cancer. *Int J Mol Sci.* 2017;18(2):367. Online First: Epub Date].
- [45] Tomar D, Prajapati P, Sripada L, et al. TRIM13 regulates caspase-8 ubiquitination, translocation to autophagosomes and activation during ER stress induced cell death. *Biochim Biophys Acta.* 2013;1833(12):3134–3144. Online First: Epub Date].
- [46] Chen Y, McMillan-Ward E, Kong J, et al. Mitochondrial electron-transport-chain inhibitors of complexes I and II induce autophagic cell death mediated by reactive oxygen species. Online First: Epub Date] *J Cell Sci.* 2007;120(Pt 23):4155–4166.

- [47] Dewaele M, Maes H, Agostinis P. ROS-mediated mechanisms of autophagy stimulation and their relevance in cancer therapy. Online First: Epub Date]] *Autophagy*. 2010;6(7):838–854.
- [48] Filomeni G, Desideri E, Cardaci S, et al. Under the ROS ... thiol network is the principal suspect for autophagy commitment. Online First: Epub Date]] *Autophagy*. 2010;6(7):999–1005.
- [49] Mijaljica D, Nazarko TY, Brumell JH, et al. Receptor protein complexes are in control of autophagy. *Autophagy*. 2012;8(11):1701–1705. Online First: Epub Date]].
- [50] Rogov V, Dötsch V, Johansen T, et al. Interactions between autophagy receptors and ubiquitin-like proteins form the molecular basis for selective autophagy. *Molecular Cell*. 2014;53(2):167–178. Online First: Epub Date]]
- [51] Klionsky DJ, Abdelmohsen K, Abe A, et al. Guidelines for the use and interpretation of assays for monitoring autophagy 3rd. *Autophagy*. 2016;12(1):1–222. Online First: Epub Date]]
- [52] Liu WJ, Ye L, Huang WF, et al. P62 links the autophagy pathway and the ubiquitin–proteasome system upon ubiquitinated protein degradation. *Cell Mol Biol Lett*. 2016;21(1):29. Online First: Epub Date]].
- [53] Kageyama S, Saito T, Obata M, et al. Negative Regulation of the Keap1-Nrf2 Pathway by a p62/Sqstm1 Splicing Variant. *Mol Cell Biol*. 2018;38(7):Online First: Epub Date]]. DOI:10.1128/MCB.00642-17.
- [54] Kobayashi A, Kang MI, Okawa H, et al. Oxidative stress sensor Keap1 functions as an adaptor for Cul3-based E3 ligase to regulate proteasomal degradation of Nrf2. *Mol Cell Biol*. 2004;24(16):7130–7139. Online First: Epub Date]].
- [55] Singh A, Misra V, Thimmulappa RK, et al. Dysfunctional KEAP1-NRF2 interaction in non-small-cell lung cancer. *PLOS Med*. 2006;3(10):e420. Online First: Epub Date]].
- [56] Best SA, Sutherland KD. “Keaping” a lid on lung cancer: the Keap1-Nrf2 pathway. *Cell cycle (Georgetown, Tex)*. 2018;17(14):1696–1707. Online First: Epub Date]].
- [57] Barrera-Rodríguez R. Importance of the Keap1-Nrf2 pathway in NSCLC: is it a possible biomarker? Online First: Epub Date]] *Biomed Rep*. 2018;9(5):375–382.
- [58] Zhang W, Feng C, Jiang H. Novel target for treating Alzheimer’s Diseases: crosstalk between the Nrf2 pathway and autophagy. *Ageing Res Rev*. 2021;65:101207. Online First: Epub Date]].
- [59] Komatsu M, Kurokawa H, Waguri S, et al. The selective autophagy substrate p62 activates the stress responsive transcription factor Nrf2 through inactivation of Keap1. *Nat Cell Biol*. 2010;12(3):213–223. Online First: Epub Date]].
- [60] Jain A, Lamark T, Sjøttem E, et al. P62/SQSTM1 is a target gene for transcription factor NRF2 and creates a positive feedback loop by inducing antioxidant response element-driven gene transcription. *J Biol Chem*. 2010;285(29):22576–22591. Online First: Epub Date]].
- [61] Ichimura Y, Kumanomidou T, Sou YS, et al. Structural basis for sorting mechanism of p62 in selective autophagy. *J Biol Chem*. 2008;283(33):22847–22857. Online First: Epub Date]].
- [62] Taguchi K, Fujikawa N, Komatsu M, et al. Keap1 degradation by autophagy for the maintenance of redox homeostasis. *Proc Natl Acad Sci USA*. 2012;109(34):13561–13566. Online First: Epub Date]].